Design of Energetic Materials Based on Asymmetric Oxadiazole

Xinghui Jin,*[a] Menghui Xiao,[a] Jianhua Zhou,[a] Guowei Zhou,[a] and Bingcheng Hu[b]

A new family of asymmetric oxadiazole based energetic compounds were designed. Their electronic structures, heats of formation, detonation properties and stabilities were investigated by density functional theory. The results show that all the designed compounds have high positive heats of formation ranging from 115.4 to 2122.2 kJ mol^{-1}. $-$N$-$ bridge/$-$N$_3$ groups played an important role in improving heats of formation while $-$O$-$ bridge/$-$NF$_2$ group made more contributions to the densities of the designed compounds. Detonation properties show that some compounds have equal or higher detonation velocities than RDX, while some other have higher detonation pressures than RDX. All the designed compounds have better impact sensitivities than those of RDX and HMX and meet the criterion of thermal stability. Finally, some of the compounds were screened as the candidates of high energy density compounds with superior detonation properties and stabilities to that of HMX and their electronic properties were investigated.

1. Introduction

High energy density compounds (HEDCs, encompassing propellants, explosives and pyrotechnics) as a type of special energy material have attracted significant attention owing to their wide applications in military and civilian. Nowadays, many works have been done in designing and synthesizing novel organic HEDCs with high densities, positive heats of formation, favorable insensitivities, excellent detonation properties, good thermal stabilities, and environmental acceptability.[1–5] One concept to design new HEDCs is to select proper parent skeletons and extra energetic substituent groups which can increase the heats of formation (ΔH_f) and densities. This is because the detonation properties were mainly depended on these two parameters. Previous research have demonstrated that $-$NF$_2$ can enhance the density while $-$N$_3$ group can improve the heats of formation apparently.[6,7] Besides, $-$NF$_2$ group can also acted as incendiary and oxidizing agent during the decomposition process of an explosive. Then the next work is to select proper backbone which possesses acceptable density and heat of formation.

Recently, many oxadiazole (especially 1,2,5-oxadiazole or bridged 1,2,5-oxadiazole) based energetic materials have been reported and most of the compounds presented excellent energetic properties, thermal stabilities and sensitivities.[8–12] Generally speaking, there are four oxadiazole isomers: 1,2,4-oxadiazole, 1,2,5-oxadiazole, 1,3,4-oxadiazole, and 1,2,3-oxadiazole (Scheme 1). Among these isomers, 1,2,5-oxadiazole has the highest heat of formation while 1,2,3-oxadiazole is unstable and reverts to the diazoketone tautomer.[13] On the other hand, a series of asymmetric 1,2,4-oxadiazole and 1,2,5-oxadiazole based energetic were synthesized and investigated by Shreeve et al.[14] Then it led to the idea that how will the energetic properties change if -NF$_2$ and -N$_3$ groups were introduced into the asymmetric 1,2,5-oxadiazole and 1,3,4-oxadiazole rings?

In attempts to meet the continuing need for improved energetic materials, 24 new asymmetric oxadiazole based energetic compounds were designed (Scheme 2) based on the above-mentioned statements. Their geometrical and electronic structures, heats of formation, detonation properties, impact sensitivities, thermal stabilities and electronic structures were systematically investigated. The present research may shine lights on the further experimental study of these high density energetic compounds including their synthesis and performance testing.

[a] Prof. X. Jin, Dr. M. Xiao, Prof. J. Zhou, Prof. G. Zhou
Key Laboratory of Fine Chemicals in Universities of Shandong, School of Chemistry and Pharmaceutical Engineering, Qilu University of Technology (Shandong Academy of Sciences), Ji'nan 250353, China
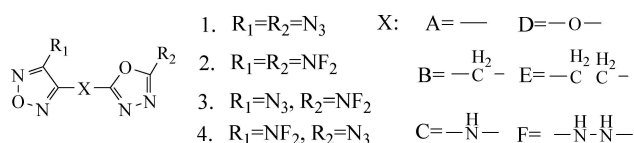E-mail: jingetiema0000@126.com

[b] Prof. B. Hu
School of Chemical Engineering, Nanjing University of Science and Technology, Nanjing, 210094, China
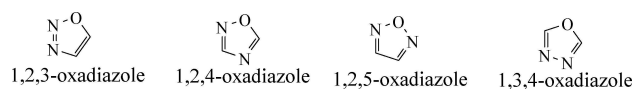
Scheme 1. Different isomers of oxadiazole.

Scheme 2. The designed energetic molecules.
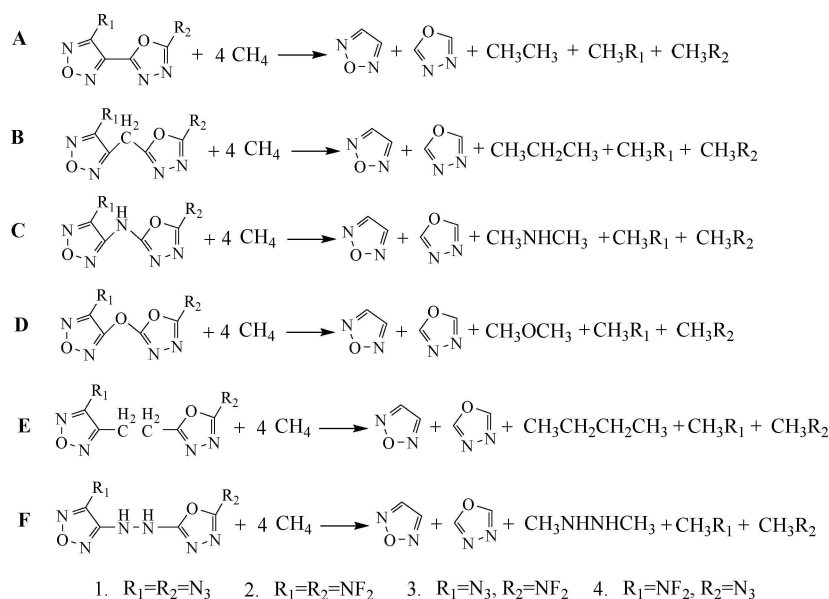
Scheme 3. The designed isodesmic reactions.

1.1. Computational Methods

All the calculations and simulation of the designed compounds were performed on Gaussian 03 program[15] combined with density functional theory (DFT) method at B3LYP/6-311G(*d,p*) level. The optimized structures were checked via vibrational analysis to ensure that they were local energy minimum on the potential energy surface. Then all the calculations (frontier molecular orbitals, heats of formation, energetic properties and bond dissociation energies) were done based on these optimized structures. The accurate gas-phase heats of formation ($\Delta H_{f,gas}$) of the title molecules were predicted by designing isodesmic reactions in which the calculation errors of $\Delta H_{f,gas}$ will decrease greatly.[16–21] The isodesmic reactions (Scheme 3) and equations (equations 1 and 2) were designed as follows:

$$\Delta H_{298K} = \sum \Delta H_{f,p} - \sum \Delta H_{f,R} \tag{1}$$

$$\Delta H_{298K} = \Delta E_{298K} + \Delta(PV) = \Delta E_0 + \Delta ZPE + \Delta H_T + \Delta nRT \tag{2}$$

Where $\Delta H_{f,p}$ and $\Delta H_{f,R}$ were ΔH_f of the products and reactants; ΔE_0 were energy changes between products and reactants; ΔZPE were difference between the zero-point energy (ZPE) of products and reactants; ΔH_T were thermal correction from 0 to 298 K; n was the number of the energetic groups; $\Delta(PV)$ equals to ΔnRT.

From the isodesmic reactions, it is found that the ΔH_f of all the related molecules were known except for CH_3NF_2, CH_3N_3, $CH_3NHNHCH_3$, 1,2,5-oxadiazole and 1,3,4-oxadiazole. Therefore, atomization reactions $C_aH_bN_cF_d \rightarrow aC(g) + bH(g) + cN(g) + dF(g)$ were employed to calculated the $\Delta H_{f,gas}$ of these unknown compounds at CBS-Q level.[22,23] The calculated total energies (E_0), zero-point energies (ZPE), thermal corrections (H_T) and gas-

phase heats of formation ($\Delta H_{f,gas}$) of the reference compounds were summarized in Table 1.

The accurate solid-phase heats of formation ($\Delta H_{f,solid}$) were also calculated according to Hess's law since energetic materials were mostly in condensed phase (equation 3).[24]

$$\Delta H_{f,solid} = \Delta H_{f,gas} - \Delta H_{sub} \tag{3}$$

where, ΔH_{sub} is the heat of sublimation. ΔH_{sub} is the sublimation enthalpy and can be calculated by the following empirical expression (equation 4).[25]

$$\Delta H_{sub} = aA^2 + b(\nu\sigma_{tot}^2)^{0.5} + c \tag{4}$$

where, a, b and c were coefficients according to the reference;[26] A was the surface area of the 0.001 e bohr^{-3} isosurface of electronic density of the molecule; ν was the

Table 1. Calculated total energies (E_0), zero-point energies (ZPE), thermal corrections (H_T) and heats of formation (ΔH_f) of the reference compounds.

Compound.	E_0 (a.u.)[a]	ZPE (kJ mol^{-1})[a]	H_T (kJ mol^{-1})[a]	$\Delta H_{f,gas}$ (kJ mol^{-1})
CH$_4$	−40.533748	117.0	10.0	−74.6[b]
CH$_3$NF$_2$	−294.298331	122.8	13.6	−98.4[c]
CH$_3$N$_3$	−204.148401	131.7	14.2	289.9[c]
CH$_3$CH$_3$	−79.856261	195.3	11.6	84.0[b]
CH$_3$CH$_2$CH$_3$	−119.180686	270.4	14.4	−104.7[b]
CH$_3$NHCH$_3$	−135.695161	254.5	14.9	−19.0[b]
CH$_3$OCH$_3$	−155.071921	208.2	13.8	−184.1[b]
CH$_3$CH$_2$CH$_2$CH$_3$	−158.504982	345.1	17.7	−125.6[b]
CH$_3$NHNHCH$_3$	−190.535853	286.9	17.1	109.3[c]
⬡	−262.161719	121.4	11.5	65.4[c]
⬡	−262.112125	119.6	11.6	197.4[c]

a, calculated at B3LYP/ 6-311G (d,p) level; b, obtained from http://webbook.nist.gov; c, calculated values were calculated at the CBS-Q level.

Table 2. Calculated HOMO and LUMO energies (eV) and energy gaps ($\Delta E_{\text{LUMO–HOMO}}$) of the designed compounds.

Compd.	A1	A2	A3	A4	B1	B2	B3	B4
HOMO	−7.44	−8.69	−7.75	−8.10	−7.29	−8.59	−7.03	−7.34
LUMO	−2.71	−3.37	−3.00	−3.08	−2.15	−2.55	−2.34	−2.19
$\Delta E_{\text{HOMO–LUMO}}$	4.73	5.32	4.75	5.02	5.14	6.04	4.69	5.15
Compd.	C1	C2	C3	C4	D1	D2	D3	D4
HOMO	−6.94	−7.87	−7.02	−7.56	−7.42	−8.57	−7.57	−8.14
LUMO	−2.14	−2.65	−2.52	−2.37	−2.38	−2.90	−2.63	−2.60
$\Delta E_{\text{HOMO–LUMO}}$	4.80	5.22	4.50	5.19	5.04	5.67	4.94	5.54
Compd.	E1	E2	E3	E4	F1	F2	F3	F4
HOMO	−7.36	−8.46	−7.44	−7.86	−6.85	−7.72	−7.01	−7.39
LUMO	−2.14	−2.55	−2.42	−2.27	−1.97	−2.39	−2.22	−2.13
$\Delta E_{\text{HOMO–LUMO}}$	5.22	5.91	5.02	5.59	4.88	5.33	4.79	5.26

degree of balance between positive and negative potential on the isosurface; σ_{tot}^2 was the measure of variability of the electrostatic potential on the molecular surface (by Multiwfn program).[27]

Detonation velocity (*D*) and detonation pressure (*P*) were two important indicators to evaluate the explosive performances of energetic materials. These parameters can be predicted by Kamlet-Jacobs equations (equation 5 and 6):[28]

$$D = 1.01(N\overline{M}^{0.5}Q^{0.5})^{0.5}(1 + 1.3\rho) \tag{5}$$

$$P = 1.558\rho^2 N\overline{M}^{0.5}Q^{0.5} \tag{6}$$

where *D* was detonation velocity (km s^{-1}); *P* was detonation pressure (GPa); *N* was the mole of detonation gases per-gram explosive (mol g^{-1}), $\overline{M}$ was average molecular weight of these gases (g mol^{-1}), *Q* was heat of detonation (cal g^{-1}) and ρ was the density which can be modified by equation 7 proposed by Politzer *et al.*:[29]

$$\rho = \beta_1\left(\frac{M}{V}\right) + \beta_2(\nu\sigma_{tot}^2) + \beta_3 \tag{7}$$

where β_1, β_2, and β_3 were coefficients according to the reference, *M* was the molecular mass (g mol^{-1}), *V* was the volume of a molecule (m^3 mol^{-1}).

Bond dissociation energies (BDEs) of the title compounds were presented to predict the strength of bonding and the way of bond cleavage. The accurate BDEs were given in terms of equation (8) and (9).

$$\text{BDE}_0(A-B) = E_0(A^\bullet) + E_0(B^\bullet) - E_0(A-B) \tag{8}$$

$$\text{BDE}(A-B)_{ZPE} = \text{BDE}_0(A-B) + \Delta E_{ZPE} \tag{9}$$

where $E_0(A^\bullet)$, $E_0(B^\bullet)$ and $E_0(A–B)$ were the energy of $A^\bullet$, $B^\bullet$ and A–B; ΔE_{ZPE} was the difference between the *ZPE*s of the products and the reactants.

Finally, impact sensitivity (h_{50}) was calculated according to equation 10 since it can reflect the stability of an energetic material during the storage or handling process.[30]

$$h_{50} = a\sigma_+^2 + b\frac{\sigma_+^2\sigma_-^2}{(\sigma_+^2 + \sigma_-^2)^2} + c \tag{10}$$

where *a*, *b* and *c* were constants; σ_+^2, σ_-^2 were indicators of the strengths and variabilities of the positive and negative surface potentials.

2. Results and Discussion

2.1. Frontier Molecular Orbitals

Frontier molecular orbitals, which contain the highest occupied molecular orbital (HOMO) and the lowest unoccupied molecular orbital (LUMO), will provide useful information in kinetic stability, chemical reactivity and optical polarizability of a molecule.[31] Table 2 presented the energy of HOMO (E_{HOMO}), the energy of LUMO (E_{LUMO}) and the energy gap ($\Delta E_{\text{LUMO-HOMO}}$) of every compound. It is found that values of E_{HOMO} and E_{LUMO} were from −8.69 eV (compound **A2**) to −6.85 eV (compound **F1**) and from −3.37 eV (compound **A2**) to −1.97 eV (compound **F1**), respectively. Obviously, compound **A2** has the lowest HOMO/LUMO energy while compound **F1** has the highest values of HOMO/LUMO energy. On the other hand, compound **B2** has the highest $\Delta E_{\text{LUMO-HOMO}}$ (6.04 eV) while compound **C3** has the smallest $\Delta E_{\text{LUMO-HOMO}}$ (4.50 eV). It indicates that compound **C3** will be more chemical reactive compared to compound **B2**.

Figure 1 displays the variation trends of E_{HOMO}, E_{LUMO} and $\Delta E_{\text{LUMO-HOMO}}$ of the title compounds. For the derivatives with the same bridges and different substituents, it is seen that series 2 have the lowest E_{HOMO} and E_{LUMO} while series 1 possess the highest values (except for compounds **B1** and **B2**). This is because the electron-withdrawing capacity of -NF$_2$ group is more stronger than that of −N$_3$ group. Compared to series 3 and 4, value of E_{HOMO} were found to be different from each other while values of E_{LUMO} were very close to each other. It indicates that the influence of different positions of the substituent groups on E_{HOMO} was apparent and the variation trend of E_{HOMO} was more obvious than E_{LUMO}. In view of the $\Delta E_{\text{LUMO-HOMO}}$, the variation trends of $\Delta E_{\text{LUMO-HOMO}}$ of series **B** and E
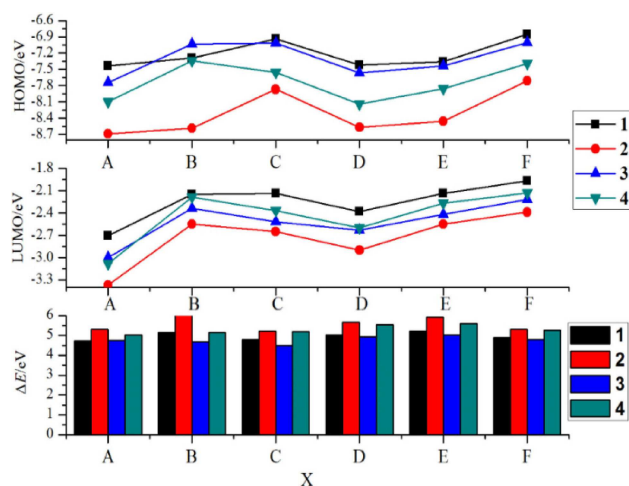
Figure 1. Variation trends of E_{HOMO}, E_{LUMO} and $\Delta E_{LUMO-HOMO}$.

were more evident compared to series **A**, **C**, **D** and **F** which suggests that the oxadiazole rings were the main impact factor for series **A**, **C**, **D** and **F**. Oppositely, energetic groups contribute more to series **B** and **E**. It is also seen that series 2 have the highest $\Delta E_{LUMO-HOMO}$ while series 3 have the lowest $\Delta E_{LUMO-HOMO}$ (except for compound **A3**). All the results indicate that both of the energetic groups and bridges will interact with the frontier molecular orbitals.

2.2. Heat of Formation and Density

Calculated total energies (E_0), thermal corrections (H_T), zero point energies (ZPE), molecular properties (A, v and σ^2_{tot}), heats

of formation (ΔH_f) and densities (ρ) of the title compounds were summarized in Table 3. Obviously, the variation trends of the gas-phase heats of formation ($\Delta H_{f,gas}$) and solid-phase heats of formation ($\Delta H_{f,solid}$) were similar to each other. High positive solid-phase heats of formation ($\Delta H_{f,solid}$) were found for all the designed compounds range from 115.4 (compound **D2**) to 2122.2 kJ mol^{-1} (compound **C1**). This result meets the concept for designing energetic materials since high positive ΔH_f plays an important role in improving the detonation properties of an explosive. On the other hand, the densities of the title compounds were from 1.60 (compound **E1**) to 2.06 g cm^{-3} (compound **D2**). For a comparison, all the compounds possess higher ΔH_f than those of RDX (79.0 kJ mol^{-1}) and HMX (102.4 kJ mol^{-1}).[32] However, only 14 compounds (**A2**, **A3**, **A4**, **B2**, **C2**, **C3**, **C4**, **D2**, **D3**, **D4**, **E2**, **F2**, **F3** and **F4**) have higher densities than that of RDX (1.82 g cm^{-3}) while 6 compounds (**A2**, **B2**, **C2**, **D2**, **D3** and **F2**) possess equal or higher densities to that of HMX (1.91 g cm^{-3}).[33]

Figure 2 illustrates the variation trends of the solid-phase heats of formation and densities of the title compounds. For the derivatives with the same bridges and different substituents, it is found that double $-N_3$ group substituted molecules have the highest $\Delta H_{f,solid}$ while the double $-NF_2$ group substituted molecules have the highest ρ. It can be concluded that $-N_3$ group was more effective in improving the $\Delta H_{f,solid}$ while $-NF_2$ group was more effective in improving values of ρ. Besides, similar $\Delta H_{f,solid}$ and ρ were found when both of $-N_3$ and $-NF_2$ groups were introduced to the oxadiazole rings at the same time. For the derivatives with the same substituents and different bridges, the $-NH-$ bridged compounds were found to have the highest $\Delta H_{f,solid}$ while the -O- bridged ones have the highest ρ. This phenomenon shows that the $-NH-$ was the most effective bridge in improving $\Delta H_{f,solid}$ while the $-O-$ bridge

Table 3. Calculated total energy (E_0), thermal correction (H_T), zero point energy (ZPE), molecular properties, heat of formation (ΔH_f) and density (ρ).

Compd.	E_0 (a.u)	ZPE (kJ mol^{-1})	H_T (kJ mol^{-1})	$\Delta H_{f,gas}$ (kJ mol^{-1})	A (Å^2)	v	σ^2_{tot} (kcal mol^{-1})^2	ΔH_{sub} (kJ mol^{-1})	$\Delta H_{f,solid}$ (kJ mol^{-1})	ρ (g cm^{-3})
A1	−850.323859	206.3	34.7	1127.3	219.4	0.247	146.8	107.8	1019.5	1.74
A2	−1030.566190	183.9	36.1	499.8	202.7	0.209	155.9	97.8	402.0	2.03
A3	−940.447866	195.3	35.3	806.2	210.1	0.244	139.8	102.1	704.1	1.88
A4	−940.443436	194.9	35.5	817.6	212.0	0.240	152.1	104.4	713.2	1.88
B1	−889.657677	281.6	38.2	914.9	239.5	0.250	137.3	117.0	797.9	1.66
B2	−1069.903822	259.0	39.6	277.1	221.1	0.185	175.1	106.4	170.7	1.93
B3	−979.782216	270.5	38.9	592.3	229.3	0.239	155.1	113.2	479.1	1.79
B4	−979.778553	270.0	39.0	601.6	232.0	0.222	152.5	112.8	488.8	1.79
C1	−905.694378	251.3	37.9	2239.8	233.3	0.233	177.3	117.6	2122.2	1.72
C2	−1085.940327	228.4	39.3	1602.2	215.0	0.145	256.7	106.2	1496.0	2.00
C3	−995.820112	239.4	38.9	1913.6	225.3	0.250	235.7	122.2	1791.4	1.86
C4	−995.815961	239.6	38.7	1924.5	225.8	0.177	199.9	110.5	1814.0	1.85
D1	−925.545383	218.2	37.2	843.1	230.6	0.250	116.0	109.0	734.1	1.77
D2	−1105.788960	195.6	38.5	212.0	212.3	0.206	116.4	96.6	115.4	2.06
D3	−1015.667381	206.2	38.1	526.6	223.3	0.250	157.5	111.5	415.1	1.91
D4	−1015.665883	206.7	38.0	530.9	223.2	0.221	115.0	102.9	428.0	1.90
E1	−928.987170	356.4	41.9	880.8	260.6	0.243	121.9	125.9	754.9	1.60
E2	−1109.234475	333.9	43.4	240.2	242.8	0.218	141.1	116.6	123.6	1.84
E3	−1019.113356	345.4	42.6	554.1	250.5	0.250	121.8	120.7	433.4	1.72
E4	−1019.108590	344.9	42.7	566.2	253.0	0.243	124.6	122.0	444.2	1.71
F1	−961.031468	295.9	41.1	1078.0	251.6	0.239	199.9	130.9	947.1	1.70
F2	−1141.278583	272.3	43.0	437.2	234.5	0.141	258.7	115.6	321.6	1.96
F3	−1051.156805	284.3	42.1	753.1	242.3	0.198	213.5	122.9	630.2	1.83
F4	−1051.153629	283.7	42.3	761.1	244.0	0.184	220.5	123.0	638.1	1.83
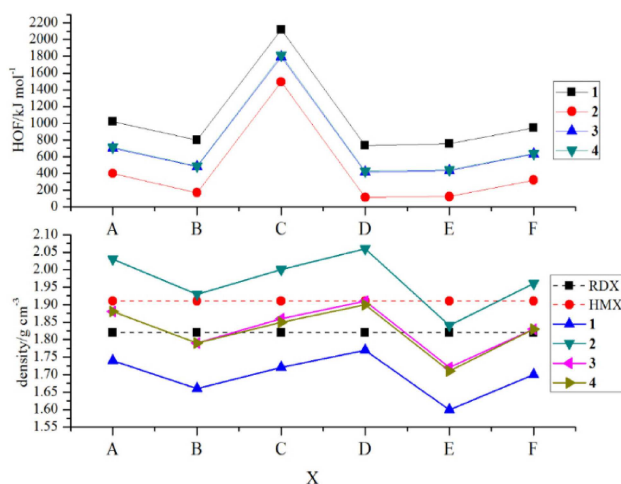
Figure 2. Variation trends of the $\Delta H_{f,solid}$ and ρ of the title compounds.

Table 4. Predicted heats of detonation (Q), detonation velocities (D), detonation pressures (P) and h_{50} of the designed compounds.

Compound	Q (cal g^{-1})	D (km s^{-1})	P (GPa)	h_{50}/cm
A1	1535.15	8.01	27.9	55.7
A2	1783.87	9.62	43.9	46.4
A3	1657.96	8.79	35.2	55.1
A4	1667.41	8.00	35.3	53.9
B1	1262.92	7.27	22.3	56.5
B2	1510.32	8.75	35.4	40.5
B3	1386.60	7.99	28.2	53.7
B4	1396.10	8.00	28.3	49.5
C1	2581.46	9.17	36.3	52.0
C2	2725.42	10.67	53.6	30.1
C3	2639.11	9.90	44.3	56.2
C4	2661.16	9.88	44.0	38.4
D1	1413.06	8.26	30.0	56.4
D2	1588.50	9.53	43.5	45.8
D3	1460.50	8.71	34.8	56.4
D4	1473.04	8.69	34.6	49.5
E1	1193.63	6.88	19.5	54.8
E2	1429.63	8.22	30.4	48.5
E3	1310.79	7.54	24.5	56.5
E4	1320.79	7.53	24.4	54.7
F1	1324.73	7.77	25.9	53.5
F2	1554.40	9.20	39.5	29.3
F3	1440.17	8.48	32.2	43.3
F4	1447.43	8.49	32.3	40.0
RDX[33]	1590.7	8.75	34.0	26[a](35)[b]
HMX[33]	1633.9	9.10	39.0	29[a](32)[b]

[a] Data From reference [34], [b]calculated at B3LYP/6-311G(d,p) level.

will improve the ρ evidently. The influence order of different bridges on $\Delta H_{f,solid}$ and ρ can be written as follows: (1) for $\Delta H_{f,solid}$, $-$NH$>$-directly link$\approx-$NHNH$->-$O$->-$CH$_2->$ $-$CH$_2$CH$_2-$; (2) for ρ, $-$O$->$ directly link$\approx-$NHNH$-\approx-$NH$->$ $-$CH$_2->-$CH$_2$CH$_2-$. Overall, variation trends of $\Delta H_{f,solid}$ and ρ were similar to each other for each series. All the results reveals that the effects of the bridged links on the $\Delta H_{f,solid}$ and ρ were coupled to those of the energetic groups.

2.3. Detonation Properties and Impact Sensitivities

Table 4 shows the heats of detonation (Q), detonation velocities (D), detonation pressures (P), impact sensitivities (h_{50}) together with those for the popular explosives RDX and HMX. It is seen that values of Q, D, P and h_{50} were presented as follows: Q were from 1193.63 (compound **E1**) to 2725.42 cal g^{-1} (compound **C2**); D were from 6.88 (compound **E1**) to 10.67 km s^{-1} (compound **C2**), P were from 19.5 (compound **E1**) to 53.6 GPa (compound
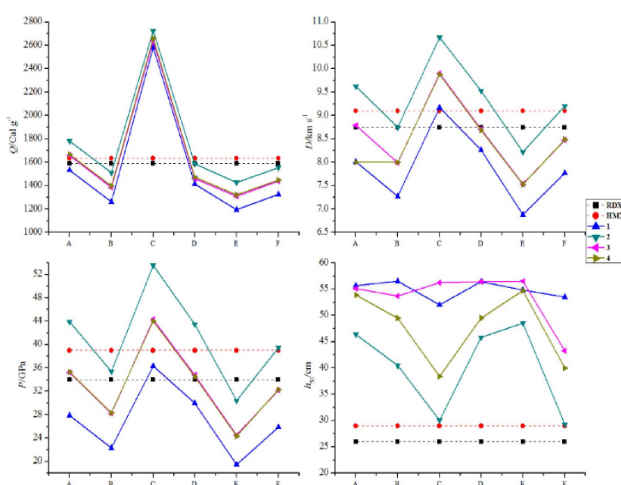

Figure 3. Variation trends of Q, D, P and h_{50} of the title compounds.

C2) and h_{50} were from 29.3 (compound **F2**) to 56.5 cm (compound **B1**), respectively. It is interesting to found that compound **C2** have the highest Q, D and P values while compound **E1** have the lowest Q, D and P values. It indicates that Q was critical to D and P. Consequently, molecules with higher values of Q will possess higher values of D and P.

Figure 3 (a–d) shows the variation trends of Q, D, P and h_{50} of the title compounds, respectively. From the figure, it is seen that variation trends of Q, D and P were approximately the same throughout the series while that of h_{50} shows no regularity. For derivatives with the same bridges and different substituents, it is found that double $-$NF$_2$ group substituted compounds have the highest values of Q, D and P while the double $-$N$_3$ group substituted ones have the lowest values. But for the molecules in which $-$N$_3$ and $-$NF$_2$ groups were introduced to the oxadiazole rings together, the values of Q, D and P were similar to each other. For the derivatives with the same substituents and different bridges, the $-$NH$-$ bridged compounds were found to have the highest Q, D and P values while the $-$CH$_2$CH$_2-$ bridged ones have the lowest values. It can be concluded that -NH- bridge will be more effective in improving Q, D and P than any other bridges. For series 1 and 4, the -NH- bridged compounds have the lowest h_{50} values while $-$NHNH$-$ bridged compounds have the lowest h_{50} values for series 2 and 3. The variation trends of series 2 and 4 were stronger than series 1 and 3 suggesting that the bridges were the most important influence factor for series 2 and 4 while the energetic groups may paly an important role in series 1 and 3. For a comparison, only 7 compounds (**A2**, **A3**, **A4**, **C1**, **C2**, **C3** and **C4**) have superior values of Q to those of RDX

(1590.7 cal g^{-1}) and HMX (1633.9 cal g^{-1}). 9 compounds (**A2**, **A3**, **B2**, **C1**, **C2**, **C3**, **C4**, **D2** and **F2**) have equal or higher values of D to RDX (8.75 km s^{-1}) while 7 compounds (**A2**, **C1**, **C2**, **C3**, **C4**, **D2** and **F2**) have higher values of D than HMX (9.10 km s^{-1}). 12 compounds (**A2**, **A3**, **A4**, **B2**, **C1**, **C2**, **C3**, **C4**, **D2**, **D3**, **D4** and **F2**) have higher values of P than RDX (34.0 GPa) while 6 compounds (**A2**, **C2**, **C3**, **C4**, **D2** and **F2**) have higher values of P than HMX (39.0 GPa). Again for h_{50}, all the designed compounds have higher h_{50} values than RDX (26 cm) and HMX (29 cm) which reveals that these compounds will be more stable under external impacts.

2.4. Thermal Stabilities

Bond dissociation energy (BDE) as an important indicator was investigated because it can provide useful information in understanding the thermally stability, elucidating the pyrolysis mechanism and bond cleavage process of an energetic compound. Some research believed that the bridge or energetic groups acted as trigger bond during the decomposition process and thus, BDEs of the possible trigger bonds were selected and investigated: (1) ring-R; (2) C—N (bridge); (3) C—O (bridge); (4) N—N (bridge); (5) C—C (bridge). The weakest bond order (BO) and the corresponding BDEs of the title compounds were summarized in Table 5. From the table, it is seen that the BDEs of ring-R, C—C bridge, C—N bridge, C—O bridge and N—N bridge ranges from 266.4 (compound **A3**) to 362.6 kJ mol^{-1} (compound **F1**), from 237.3 (compound **E1**) to 518.9 kJ mol^{-1} (compound **A1**), from 342.2 (compound **F1**) to 400.3 kJ mol^{-1} (compound **C3**), from 240.6 (compound **D3**) to 266.1 kJ mol^{-1} (compound **D4**) and from 132.4 (compound **F1**) to 154.6 kJ mol^{-1} (compound **F2**), respectively. It is also interesting to note that compound F1
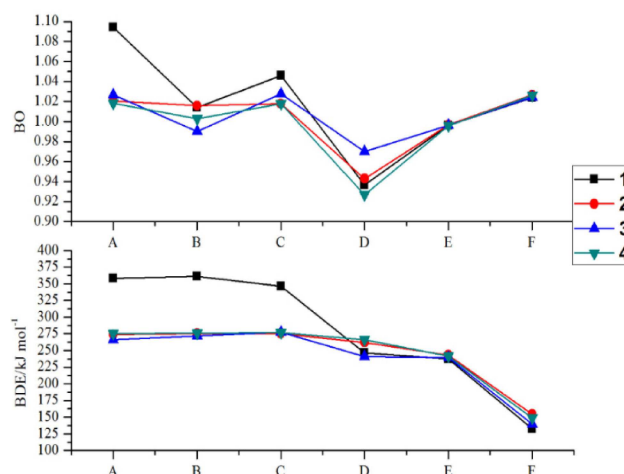

Figure 4. The variation trends of BO and BDE of the designed compounds.

not only has the highest BDEs of ring-R bond, but also possesses the lowest BDEs of N—N bond. The result shows that the effects of the bridged links on the BDEs values of the designed compounds were coupled to those of the substituted energetic groups.

Figure 4 displays the variation trends of BO and BDEs of the designed compounds. For series 2–4, the —O— bridged compounds have the lowest values of BO while the -NHNH- bridged compounds have the highest values of BO. BO of the directly link, —CH$_2$—, —NH— and —O— bridged compounds were also found to be fluctuated evidently than those of —NHNH— and —CH$_2$CH$_2$— bridged ones. It indicates that the types of bridges played an important role in BO for series **A**--**D** while energetic groups acted as the main influence factor for series **E** and **F**. In

| Compd.	ring-R BO	BDE	C—C(bridge) BO	BDE	C—N(bridge) BO	BDE	C—O(bridge) BO	BDE	N—N (bridge) BO	BDE
Table 5. Bond dissociation energies (BDE, kJ mol^{-1}) for the weakest bonds of the designed compounds.										
A1	1.0941	358.5	1.0635	518.9	–	–	–	–	–	–
A2	1.0206	273.9	1.0507	514.1	–	–	–	–	–	–
A3	1.0268	266.4	1.0555	517.5	–	–	–	–	–	–
A4	1.0182	275.6	1.0613	518.8	–	–	–	–	–	–
B1	1.0139	361.4	0.9860	372.6	–	–	–	–	–	–
B2	1.0160	275.5	1.0100	377.5	–	–	–	–	–	–
B3	0.9903	272.1	0.9846	372.6	–	–	–	–	–	–
B4	1.0028	275.8	0.9881	375.6	–	–	–	–	–	–
C1	1.0900	346.8	–	–	1.0457	346.6	–	–	–	–
C2	1.0179	275.6	–	–	1.0525	360.7	–	–	–	–
C3	1.0275	277.1	–	–	1.0720	400.3	–	–	–	–
C4	1.0178	276.4	–	–	1.0351	361.1	–	–	–	–
D1	1.0915	353.7	–	–	–	–	0.9366	246.4	–	–
D2	1.0185	274.4	–	–	–	–	0.9430	262.3	–	–
D3	1.0277	269.0	–	–	–	–	0.9698	240.6	–	–
D4	1.0176	275.1	–	–	–	–	0.9271	266.1	–	–
E1	1.0762	361.8	0.9962	237.3	–	–	–	–	–	–
E2	1.0150	276.4	0.9967	243.2	–	–	–	–	–	–
E3	1.0239	275.4	0.9964	239.7	–	–	–	–	–	–
E4	1.0145	276.6	0.9960	241.6	–	–	–	–	–	–
F1	1.0763	362.6	–	–	1.0851	342.2	–	–	1.0241	132.4
F2	1.0189	276.9	–	–	1.0930	345.0	–	–	1.0266	154.6
F3	1.0281	274.6	–	–	1.0986	344.9	–	–	1.0245	139.3
F4	1.0189	277.4	–	–	1.0790	343.5	–	–	1.0264	148.9
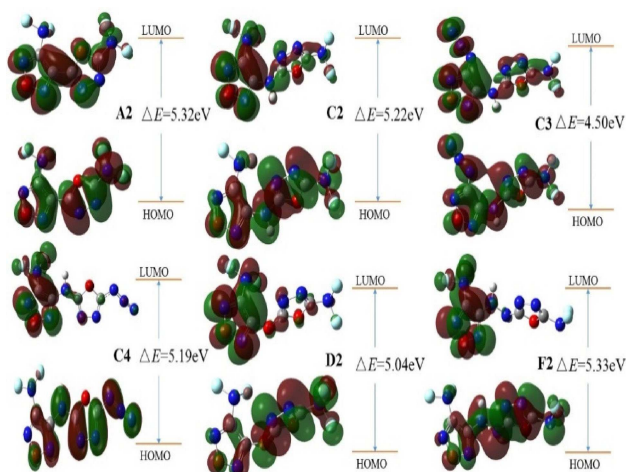
Figure 5. Distribution of LUMO and HOMO of the selected compounds.

view of BDEs, the -NHNH- bridged compounds have the lowest BDE values which suggests that the introduction of —NHNH— bridge may decrease the thermal stability of the designed compounds. For series 1, the BDEs decease sharply when the oxadiazoles were linked by —O—, —NHNH— and —CH_2CH_2— bridges. In addition, the variation trends can be negligible of series for series 2–4 when the bridges were directly link, —NH—, —O—, —CH_2— and —CH_2CH_2—. Finally, compound **A1** has the highest BO (1.0941) while compound **D4** has the lowest BO (0.9271). But on the contrary, compound **B1** has the highest BDE value 361.4 (kJ mol⁻¹) while compound **F1** has the lowest BDE value (132.4 kJ mol⁻¹). The phenomenon reveals that, for different chemical bonds, there exists no inevitable relation between the values of BOs and BDEs.

A potential high energy density compound should not only meet the standard of detonation properties (usually compared to those of RDX or HMX), but also should have excellent thermal stabilities.[35] Take both of detonation properties and thermal stabilities into consideration, 6 compounds (**A2**, **C2**, **C3**, **C4**, **D2** and **F2**) were screened as the candidates of high energy density compounds which possess superior detonation properties and thermal stabilities to that of HMX.

2.5. Electronic Structures

Electronic structures (such as distribution of LUMO and HOMO, electrostatic potential (ESP) and contour line maps) of the selected compounds (**A2**, **C2**, **C3**, **C4**, **D2** and **F2**) were fully investigated. Figure 5 presents the distribution of LUMO and HOMO of the selected compounds. It is seen that the distribution of HOMO and LUMO of compounds **A2**, **C2** and **C3** were mainly localized both on 1,3,4-oxadiazole and 1,2,5-oxadiazole rings while compounds **C4**, **D2** and **F2** were on the opposite side. The fact is that LUMOs were mainly distributed on the 1,2,5-oxadiazole ring whereas the HOMO were mainly distributed on the 1,3,4-oxadiazole ring. In addition, the energy gaps of these compounds **A2**, **C2**, **C3**,

C4, **D2** and **F2** were 5.32, 5.22, 4.50, 5.19, 5.04 and 5.33 eV, respectively. It implies that the predicted sequence of stabilities was **F2** > **A2** > **C2** > **C4** > **D2** > **C3** which is also the reverse order of the chemical activities. On the other hand, the HOMO and LUMO distributions agree well with the NBOs that calculated at the same level. Take compound **C4** for example, the NBO charges that distributed on HOMO was about −0.0707 while NBO charges that distributed on LUMO was about 0.0707 (the detailed information on chemical structure and NBO charges of compound **C4** can be found in the supporting information). Obviously, HOMO acted as electron donor while LUMO acted as electron acceptor.

Electrostatic potential (ESP) of the selected compounds were investigated since it is an important part to predict the intermolecular interaction, charge distributions, and chemical reactivity sites on molecular surfaces.[36, 37] 3D plots of ESP and ratios of the positive and negative areas (green color presents the positive potential and red color presents the negative potential) were visualized in Figure 6. For compound **A2**, positive potentials were mainly concentrated on the oxadiazole rings while the negative potentials were mainly concentrated on the energetic groups. For compounds **C2-F2**, these potentials were relatively decentralized: positive potentials localized on parts of the oxadiazole rings, bridges and -N_3 groups while negative potentials localized on -NF_2 groups, oxygen and nitrogen atoms of the oxadiazole rings. In addition, the global maxima ESPs of compounds **A2**, **C2**, **C3**, **C4**, **D2** and **F2** were calculated as 39.8, 65.2, 60.8, 56.9, 38.9 and 61.6 kcal mol⁻¹ while the global minima ESP were calculated as −25.4, −28.8, −25.8, −43.1, −25.0 and 29.4, respectively.

These sites with the most positive potentials maybe attacked easily by the nucleophile. In view of the surface area of positive and negative potentials, it is found that the area ratio of positive potentials of the selected compounds were larger than the area ratio of negative potentials which indicates that the electrostatic potential is mainly contributed by nuclear charges.
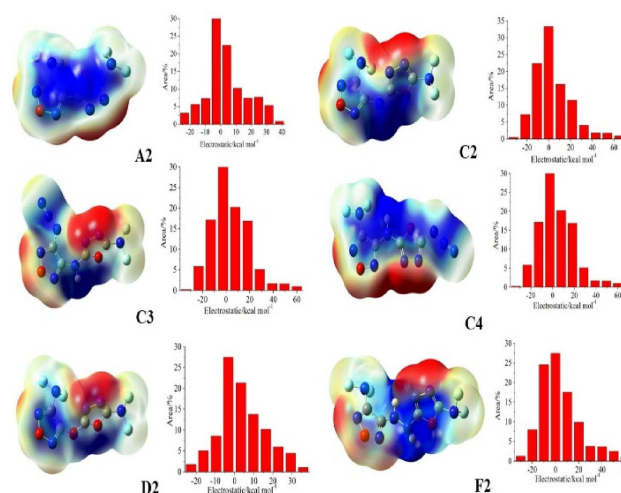

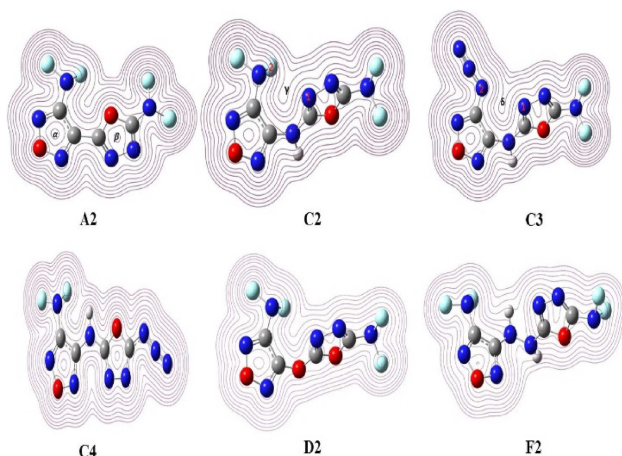**Figure 6.** ESP and ratios of the positive and negative potentials.

Figure 7. Contour line maps of the selected compounds.

The contour line maps of the electronic densities on compounds **A2**, **C2**, **C3**, **C4**, **D2** and **F2** were plotted in Figure 7. It also should be pointed out that high peaks correspond to the nuclear charge of heavy nucleus which will improve the electron aggregation. It is seen that the electron densities around the fluorine atoms were the highest due to its strong electron absorption effects while electron densities around the hydrogen atoms were the lowest. Delocalization was observed in the oxadiazole rings (for example, compound **A2**, regions α and β) and this phenomenon may improve the stability of the ring skeleton and the molecular structure. Besides, electronic density was also found to be reduced in regions γ (compound **C2**) and δ (compound **C3**) which may be caused by the repulsive interactions of heavy atoms (compound **C2**, N1…F2; compound **C3**, N1…N2).

3. Conclusions

A series of new energetic materials based on asymmetric oxadiazole were designed and investigated. The results show that all the designed compounds have high positive heats of formation range from 115.4 to 2122.2 kJ mol^{-1} and $-$N$-$bridge/$-$N$_3$ group were the most effective factors in improving heats of formation of the designed compounds. Densities were in the range of 1.60–2.06 g cm^{-3} and $-$O$-$ bridge/$-$NF$_2$ groups make more contributions to densities of the designed compounds. Values of detonation velocities and detonation pressures range from 6.88 to 10.67 km s^{-1} and from 19.5 to 53.6 GPa, respectively. Besides, all the designed compounds have better impact sensitivities than those of RDX and HMX and meet the criterion of thermal stability. Take both of detonation properties and thermal stabilities into consideration, 6 compounds (**A2**, **C2**, **C3**, **C4**, **D2** and **F2**) were selected as the candidates of high energy density compounds.

Conflict of Interest

The authors declare no conflict of interest.

[1] C. Zhang, C. G. Sun, B. C. Hu, C. M. Yu, M. Lu, *Science* **2017**, *355*, 355–374.

[2] X. H. Jin, M. H. Xiao, C. Y. Wang, C. Zhang, J. H. Zhou, B. C. Hu, *Eur. J. Org. Chem.* **2019**, *5*, 988–994.

[3] Y. X. Tang, L. A. Mitchell, G. H. Imler, D. A. Parrish, J. M. Shreeve, *Angew. Chem. Int. Ed.* **2017**, *56*, 5894–5898; *Angew. Chem.* **2017**, *129*, 5988–5992.

[4] T. G. Witkowski, E. Sebastiao, B. Gabidullin, A. G. Hu, F. Zhhang, M. Murugesu, *ACS Appl. Energy Mater.* **2018**, *1*, 589–593.

[5] Y. Qu, S P. Babailov, *J. Mater. Chem. A* **2018**, *6*, 1915–1940.

[6] J. Q. Yang, G. X. Wang, X. D. Gong, J. G. Zhang, Y. A. Wang, *ACS Omega* **2018**, *3*, 9739–9745.

[7] X. H. Jin, M. H. Xiao, G. W. Zhou, J. H. Zhou, B. C. Hu, *RSC Adv.* **2019**, *9*, 5417–5430.

[8] T. M. Klapötke, T. G Witkowski, *Propellants Explos. Pyrotech.* **2015**, *40*, 366–373.

[9] M. A. Kettner, T. M. Klapötke, *Chem. Commun.* **2014**, *50*, 2268–2270.

[10] Y. X. Tang, H. X. Gao, L. A. Mitchell, D. A. Parrish, J. M. Shreeve, *Angew. Chem. Int. Ed.* **2016**, *128*,1159-1162.

[11] V. Thottempudi, J. H. Zhang, C. L. He, J. M. Shreeve, *RSC Adv.* **2014**, *92*, 50361–50364.

[12] T. M. Klapötke, T. G. Witkowski, *ChemPlusChem* **2016**, *81*, 357–360.

[13] J. A. Joule, K. Mills, G. F. Smith, *Heterocyclic Chemistry*, 3rd ed., Taylor & Francis, New York 1995.

[14] H. Wei, C. L. He, J. H. Zhang, J. M. Shreeve, *Angew. Chem. Int. Ed.* **2015**, *54*, 9367–9371; *Angew. Chem.* **2015**, *127*, 9499–9503.

[15] M. J. Frisch, G. W. Trucks, H. B. Schlegel, G. E. Scuseria, M. A. Robb, J. R. Cheeseman, J. A. Montgomery, T. Vreven, K. N. Kudin, J. C. Burant, J. M. Millam, S. S. Iyengar, J. Tomasi, V. Barone, B. Mennucci, M. Cossi, G. Scalmani, N. Rega, G. A. Petersson, H. Nakatsuji, M. Hada, M. Ehara, K. Toyota, R. Fukuda, J. Hasegawa, M. Ishida, T. Nakajima, Y. Honda, O. Kitao, H. Nakai, M. Klene, X. Li, J. E. Knox, H. P. Hratchian, J. B. Cross, C. Adamo, J. Jaramillo, R. Gomperts, R. E. Stratmann, O. Yazyev, A. J. Austin, R. Cammi, C. Pomelli, J. W. Ochterski, P. Y. Ayala, K. Morokuma, G. A. Voth, P. Salvador, J. J. Dannenberg, V. G. Zakrzewski, S. Dapprich, A. D. Daniels, M. C. Strain, O. Farkas, D. K. Malick, A. D. Rabuck, K. Raghavachari, J. B. Foresman, J. V. Ortiz, Q. Cui, A. G. Baboul, S. Clifford, J. Cioslowski, B. B. Stefanov, G. Liu, A. Liashenko, P. Piskorz, I. Komaromi, R. L. Martin, D. J. Fox, T. Keith, M. A. Al-Laham, C. Y. Peng, A. Nanayakkara, M. Challacombe, P. M. W. Gill, B. Johnson, W. Chen, M. W. Wong, C. Gonzalez, J. A. Pople, Gaussian 03, Gaussian Inc, Pittsburgh, PA **2003**.

[16] X. H. Jin, M. H. Xiao, Y. Q. Ding, J. H. Zhou, B. C. Hu, *ChemistrySelect* **2018**, *40*, 11160–11166.

[17] C. Qi, S. H. Li, Y. C. Li, T. Wang, X. K. Chen, S. P. Pang, *J. Mater. Chem.* **2011**, *21*, 3221–3225.

[18] V. D. Ghule, R. Sarangapani, P. M. Jadhav, S. P. Tewari, *J. Mol. Model.* **2011**, *17*, 1507–1515.

[19] D. Srinivas, V. D. Ghule, K. Muralidharan, H. D. B. Jenkins, *Chem. Asian J.* **2013**, *8*, 1023–1028.

[20] X. H. Li, R. Z. Zhang, X. Z. Zhang, *J. Hazard. Mater.* **2010**, *183*, 622–631.

[21] Y. Pan, J. S. Li, B. B. Cheng, W. H. Zhu, H. M. Xiao, *Comput. Theor. Chem.* **2012**, *992*, 110–119.

[22] W. H. Zhu, C. C. Zhang, T. Wei, H. M. Xiao, *Struct. Chem.* **2011**, *22*, 149–159.

[23] X. H. Li, Z. R. Zhang, X. Z. Zhang, *Struct. Chem.* **2013**, *24*, 393–400.

[24] P. W. Atkins, *Physical chemistry*, 2nd edn. Oxford University Press: Oxford **1982**.

[25] P. Politzer, Y. Ma, P. Lane, M. C. Concha, *Int. J. Quantum Chem.* **2005**, *105*, 341–347.

[26] E. F. C. Byrd, B. M. Rice, *J. Phys. Chem. A* **2006**, *110*, 1005–1013.

[27] T. Lu, F. Chen, *J. Comput. Chem.* **2012**, *33*, 580–592.

[28] M. J. Kamlet, S. J. Jacobs, *J. Chem. Phys.* **1968**, *48*, 23–25.

[29] P. Politzer, J. Martinez, J. S. Murray, M. C. Concha, *Mol. Phys.* **2009**, *107*, 2095–2101.

[30] M. Pospíšil, P. Vávra, M. C. Concha, J. S. Murray, P. Politzer, *J. Mol. Model.* **2010**, *16*, 895–901.

[31] M. Govindarajan, S. Periandy, Carthigayen, *Spectrochim. Acta Part A* **2012**, *97*, 411–422.

[32] B. M. Rice, S. V. Pai, J. Hare, *Combust. Flame* **1999**, *118*, 445–458.

[33] Y. Pan, W. H. Zhu, H. M. Xiao, *J. Mol. Model.* **2012**, *18*, 3125–3138.

[34] B. M. Rice, J. J. Hare, *J. Phys. Chem. A* **2002**, *106*, 1770–1783.

[35] G. S. Chung, M. W. Schmidt, M. S. Gordon, *J. Phys. Chem. A* **2000**, *104*, 5647–5650.

[36] P. Politzer, J. Martinez, J. S. Murray, M. C. Concha, A. Toro-Labbe, *Mol. Phys.* **2009**, *107*, 2095–2101.

[37] J. S. Murray, P. Politzer, *Comp. Mol. Sci.* **2011**, *1*, 153–163.